JOINT INSTITUTE FOR NUCLEAR RESEARCH
Bogoliubov Laboratory of Theoretical Physics (BLTP)

FINAL REPORT ON THE INTEREST PROGRAMME

Numerical simulations for IV-characteristics and magnetic moment dynamics for φ_0 Josephson junction

Supervisor:
Dr Majed Nashaat
BLTP, JINR, Dubna, Russia

Student:
Ashutosh Gupta, India
Indian Institute of Technology, Delhi
(IIT Delhi)

Participation period:
February 13 – April 2, 2023 Wave 8

Dubna, 2023

Table of Contents

Abstract …… 2

1. Simulation of Josephson Junction

    1.1 Introduction …… 3
    1.2 Josephson Junction Model…… 3
    1.3 Results …… 6
        1.3.1 Effects of model parameter on phase dynamics of Josephson Junction …… 6
        1.3.2 Effects of External Radiation …… 8

2. SFS Junction

    2.1 Introduction …… 9
    2.2 Model ……... 9
    2.3 Results …… 11

3. Conclusion …… 13

4. Acknowledgment …… 13

5. References …… 14

Abstract

Spintronics is a growing field of research and recent advancement in it has many important applications. Josephson junctions offer a promising platform for the development of spintronic devices, which have applications in information processing, data storage, and sensing, like quantum computing, spin filters, spin valves, MRI etc. Overall, future research on Josephson junctions has the potential to lead to breakthroughs in quantum computing, energy conversion, sensing, and fundamental science. In first part, we consider superconducting-insulator-superconducting (SIS) Josephson junction, and investigate the effect of junction capacitance, cases of overdamped and underdamped Josephson junction , and external radiation on the junction IV-curves. In the later part, we consider the superconducting-ferromagnetic-superconducting (SFS) Josephson junction. We examined the magnetization trajectory of different planes, IV characteristics at different values of magnetic energy relation and the spin-orbit coupling. Overall SFS Josephson junctions have potential applications in superconducting electronics, such as qubits for quantum computing and spintronics and there is a scope for researchers to optimize and control the properties of the ferromagnetic layer more precisely.

1. Simulation of Josephson Junction

1.1 Introduction

Josephson Junctions are a type of electronic device consisting of two superconducting electrodes separated by a thin insulating barrier. It was first discovered by Brian Josephson in 1962, and his discovery led him to be awarded the Nobel Prize in Physics in 1963 [1]. The functioning of a Josephson junction is based on the Josephson effect, which is the observation of the flow of electric current through a weak link between two superconductors, even in the absence of any applied voltage. This effect arises due to the wave-like nature of the electrons in the superconducting materials and their ability to tunnel through the insulating barrier. When a voltage is applied across the Josephson junction, a supercurrent can flow through the barrier. This supercurrent is made up of pairs of electrons known as Cooper pairs [2], which can travel through the insulating barrier due to quantum tunnelling. An interesting case of Josephson Junction is the superconductor-ferromagnet-superconductor (SFS) junction [3]. The ferromagnetic layer in an SFS junction can act as a spin filter, selectively allowing electrons with specific spin orientations to tunnel through the junction, while blocking others. This spin-selective tunnelling effect is due to the difference in the density of states of the two superconductors, which is modified by the presence of the ferromagnetic layer. The Josephson junction is known for its ability to create and detect very small voltages and currents, and because of this, it is used in diverse applications such as SQUIDs (superconducting quantum interference devices), which are used to measure extremely small magnetic fields. They also have potential in quantum computing, due to their ability to create and control entangled quantum states, which could be used for quantum information processing.

1.2 Josephson Junction Model

In our study, we examined a Superconductor-Insulator-Superconductor (SIS) Josephson Junction, with a current source driving a current through the junction. We have made the assumption of a homogenous supercurrent density allowing a one-dimensional treatment.

We use the RCSJ, resistivity and capacitively shunted junction, model (Figure 1). This model models the Josephson junction as three parallel circuits; a capacitor to simulate the geometrically induced capacitance between the electrodes in the junction, a resistance to account for dissipation when we have a finite voltage and, the Josephson junction itself in its ideal version.

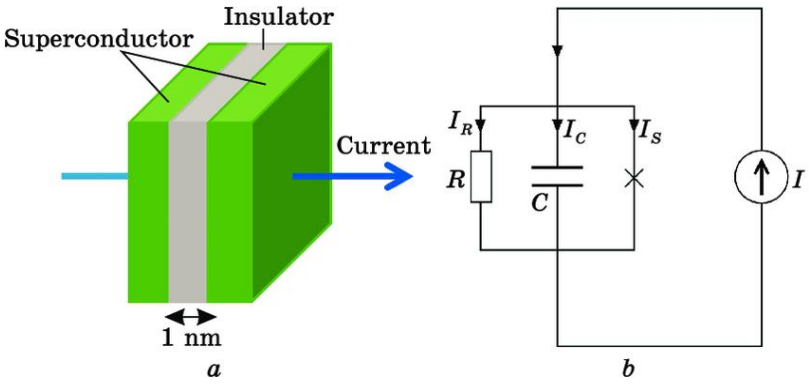

Figure 1: Josephson SIS junction with an insulating layer (a) and its equivalent RCSJ circuit (b) [4]

Kirchhoff's law states that the total current out is the same as the total current in at a junction, hence, a total current in I will split between the three parallel components dependent on their type, where I_{res} is the current through the resistor, I_{cap} is the current through the capacitor while I_{tun} is the current through the tunneling device [5].

$$I = I_{res} + I_{cap} + I_{tun}$$

We know that $I_{res} = \frac{V}{R}$ due to quasi-static particle, for the current through capacitor $\mathrm{Q} = \mathrm{CV} \rightarrow \frac{\mathrm{dQ}}{dt} = \mathrm{C}\frac{\mathrm{dV}}{dt} \rightarrow \mathrm{I}_{cap} = \mathrm{C}\frac{\mathrm{dV}}{dt}$, and the tunnelling current $\mathrm{I}_{tun} = I_c \sin(\varphi)$. Equating all the terms in the above current equation we get,

$$I = \frac{V}{R} + C\frac{dV}{dt} + I_c \sin\varphi$$

Combining this equation obtained by Kirchhoff's law, with the Josephson's voltage-phase relation as follow,

$$\frac{d\varphi}{dt} = \frac{2e}{\hbar}V$$

Normalizing the system of equations, using following parameters with time τ and voltage V_0 with plasma frequency [6]

$$V_0 = \frac{\hbar\omega_p}{2e}, \tau = \omega_p t$$

$$\omega_p = \sqrt{\frac{2eI_c}{C\hbar}}\ (plasma\ frequency), \qquad \frac{I}{I_c} \to I, \qquad \frac{V}{V_0} \to V$$

$$\beta = \frac{1}{R}\sqrt{\frac{\hbar}{2eI_cC}} = \frac{1}{\sqrt{\beta_C}}$$

Therefore obtaining,

$$\frac{d\varphi}{dt} = V$$

$$\frac{dV}{dt} = I - \sin\varphi - \beta V$$

If we consider Josephson Junction under external radiation, then the system follows additional current $I_{rad} = Asin(\omega t)$, the above system of equations become,

$$\frac{d\varphi}{dt} = V$$

$$\frac{dV}{dt} = I - \sin\varphi - \beta V + Asin(\omega t)$$

where A is the amplitude of the external radiation, and ω is its angular frequency. The above system of equations was solved using fourth order Runge–Kutta method [6].

$$\varphi^{j+1} = \varphi^j + \Delta\varphi^j$$

$$\Delta\varphi^j = \frac{1}{6}\left(P_1^j + 2P_2^j + 2P_3^j + P_4^j\right)$$

$$V^{j+1} = V^j + \Delta V^j$$

$$\Delta V^j = \frac{1}{6}\left(K_1^j + 2K_2^j + 2K_3^j + K_4^j\right)$$

where, the First Runge-Kutta coeffiecients is given by

$$P_1 = V h_t$$

$$K_1 = \{I - \sin\varphi\}\mathrm{h}_t - \beta P_1$$

Second Runge–Kutta coefficients given by,

$$P_2 = \left\{V + \frac{K_1}{2}\right\} h_t$$

$$K_2 = \left\{I - \sin\left(\varphi + \frac{P_1}{2}\right)\right\}\mathrm{h}_t - \beta P_2$$

Third Runge–Kutta coefficients given by,

$$P_3 = \left\{V + \frac{K_2}{2}\right\} h_t$$

$$K_3 = \left\{I - \sin\left(\varphi + \frac{P_2}{2}\right)\right\}\mathrm{h}_t - \beta P_3$$

and Fourth Runge–Kutta coefficients given by,

$$P_4 = \{V + K_3\} h_t$$

$$K_4 = \{I - \sin(\varphi + P_3)\}\mathrm{h}_t - \beta P_4$$

A C++ code was written to solve the system of second-order differential equation. From this solution, the instantaneous voltage is plotted as a function of external current.

1.3 Results

1.3.1 Effects of model parameter on phase dynamics of Josephson Junction

We observed the graph plotted in figure 2, when observing the current-voltage characteristics (IVC) for underdamped and overdamped Josephson junction [7]. For underdamped Josephson junctions ($\beta \ll 1$), the junction capacitance and the resistance are large, and the damping η is small. In contrast, for the overdamped junctions ($\beta \gg 1$), the junction capacitance, resistance are small, and the damping η is large.

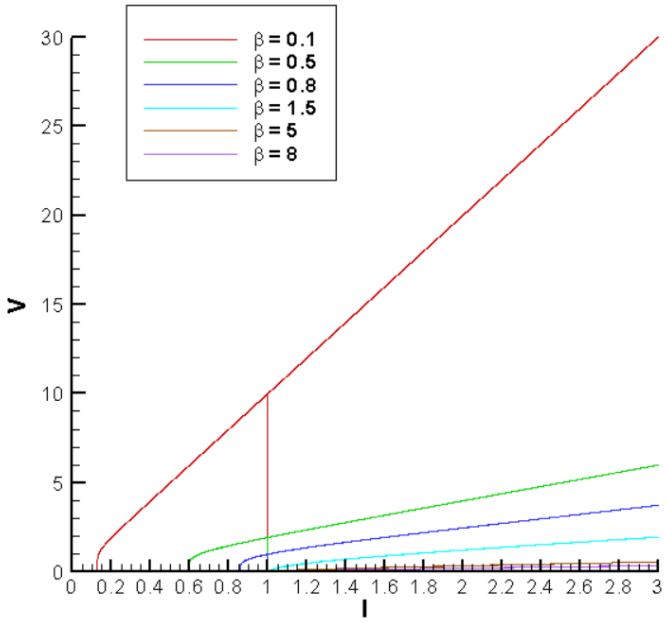

Figure 3: The current-voltage characteristics (IVC) plot for different values of β

For an underdamped Josephson junction, the voltage will depend on the current applied through the Josephson junction. If the initial current starts below the critical current Ic, the circuit will be superconducting, and therefore there will be no resistance and no voltage drop. Whereas, if the current is above I_c there will be resistance, but even if the current were to drop below I_c, there will still be resistance until the current has dropped off sufficiently. A hysteresis plot is observed as shown above. For overdamped Josephson junction, the solution will be imaginary for $I < I_c$ and linear and real for $I \gg I_c$, An imaginary voltage means that the voltage will be 90 degrees ahead of the current peak in a phase diagram. For DC current these yields, a zero net voltage for $I < Ic$. No hysteresis is observed in this overdamped case.

1.3.2 Effects of External Radiation

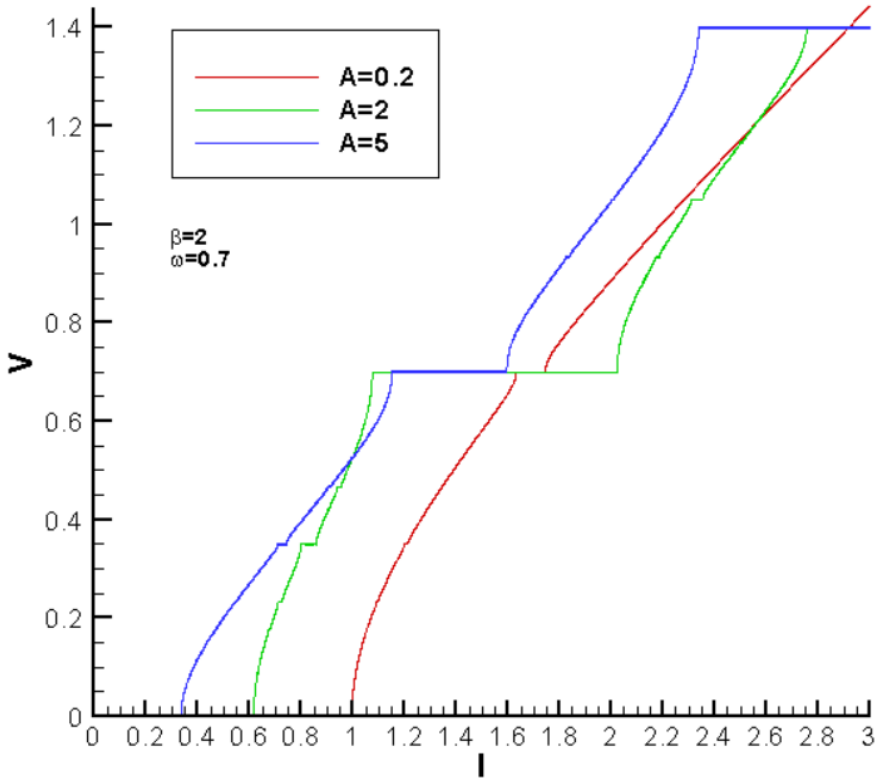

Figure 4: Appearance of Shapiro steps in current-voltage characteristics (IVC)

One interesting effect observed in the plot of external radiation is the appearance of Shapiro steps in superconducting materials. Shapiro steps [8] are a series of voltage steps that appear in the current-voltage characteristic of a superconductor when it is irradiated with microwave radiation. The steps occur at integer multiples of the frequency of the radiation, and their appearance is due to the interaction between the radiation and the superconducting electrons in the material. The Shapiro steps are quantized voltage steps and that they occur at discrete voltage values that are proportional to the frequency of the microwave radiation. For a specific n, the width of the Shapiro step is given by,

$$\Delta I = I_c \left| J_n \left(\frac{2\pi A}{\Phi \omega} \right) \right|$$

where J_n is the nth order Bessel function.

2. SFS Junction

2.1 Introduction

A superconducting-ferromagnetic-superconducting (SFS) Josephson junction is a type of Josephson junction where the barrier between two superconductors is a thin layer of ferromagnetic material. The SFS Josephson junction [9] exhibits interesting properties such as a critical current that depends on the relative orientation of the magnetization of the ferromagnetic layer with respect to the direction of the supercurrent flow. This is known as the $0-\pi$ transition, and it is due to the interplay between the singlet and triplet superconducting correlations that arise in the ferromagnetic layer. The current-phase relation (CPR) of these junctions is given by $I = I_c \sin(\varphi - \varphi_0)$, where the phase shift φ_0 is proportional to the magnetic moment perpendicular to the gradient of the asymmetric spin-orbit potential.

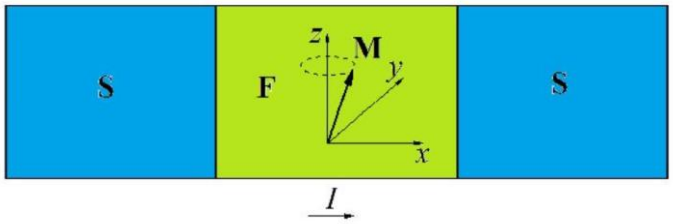

Figure 5: Schematic view of SFS Josephson junction. The external current applied along x-direction, ferromagnetic easy axis along z direction [10]

2.2 Model

In Josephson junctions with a thin ferromagnetic layer the superconducting phase difference and magnetization of the F layer are two coupled dynamical variables. The Landau-Lifshitz-Gilbert (LLG) equation [11] and Josephson relations for current and phase difference are used to derive the system of equations that describes the dynamics of these variables. The magnetization dynamics of our system are specifically given by the Landau-Lifshitz-Gilbert equation, where the effective field relies on the phase difference. It is given as following equation,

$$\frac{d\mathbf{M}}{dt} = -\gamma \mathbf{M} \times \mathbf{H}_{\text{eff}} + \frac{\alpha}{M_0}\left(\mathbf{M} \times \frac{d\mathbf{M}}{dt}\right)$$

$$\mathbf{H}_{\text{eff}} = \frac{K}{M_0}\left[Gr\sin\left(\varphi - r\frac{M_y}{M_0}\right)\hat{\mathbf{y}} + \frac{M_z}{M_0}\hat{\mathbf{z}}\right]$$

where $G = E_J/(Kv)$ is the ratio of the Josephson energy to the magnetic one where K is the anisotropic energy term, v is the volume of the ferromagnetic layer, γ is the gyromagnetic ratio, α is a phenomenological damping constant, φ is the phase difference between the superconductors across the junction. Based on the equations for Josephson junction and the magnetic system, we write the total system of equations as follows,

$$\dot{m}_x = \frac{\omega_F}{1+\alpha^2}\{-m_y m_z + \mathrm{Grm}_z \sin(\varphi - rm_y) - \alpha[m_x m_z^2 + Grm_x m_y \sin(\varphi - rm_y)]\}$$

$$\dot{m}_y = \frac{\omega_F}{1+\alpha^2}\{m_x m_z - \alpha[m_y m_z^2 - Gr(m_z^2 + m_x^2)\sin(\varphi - rm_y)]\}$$

$$\dot{m}_z = \frac{\omega_F}{1+\alpha^2}\{-Grm_x \sin(\varphi - rm_y) - \alpha[Grm_y m_z \sin(\varphi - rm_y) - m_z(m_x^2 + m_y^2)]\}$$

$$\frac{dV}{dt} = \frac{1}{\beta_c}[I - V - \sin(\varphi - rm_y)], \qquad \frac{d\varphi}{dt} = V$$

where β_c is the McCumber parameter, $m_i = M_i/M_0$ for $i = x, y, z$ is the normalized magnetization, $m_i = M_i/M_0$ for $i = x, y, z$ is the effective field normalized to K/M_s, $\omega_F = \Omega_F/\omega_C$ here the ferromagnetic resonance frequency $\Omega_f = \gamma K/M_0$ and the characteristic junction frequency $\omega_c = 2eRI_c/\hbar$ and we normalize time in unites of ω_c^{-1}, current in units of I_c, and the voltage in unites of $I_c R$ [12].

This system of equations was solved numerically using the fourth-order Runge-Kutta method and it yields $m_i(t), V(t)$, and $\varphi(t)$ as a function of the external bias current I. We observed current-voltage characteristics (IVC) at fixed system parameters and investigate the dynamics of magnetization along the IV curve by writing a C++ code.

2.3 Results

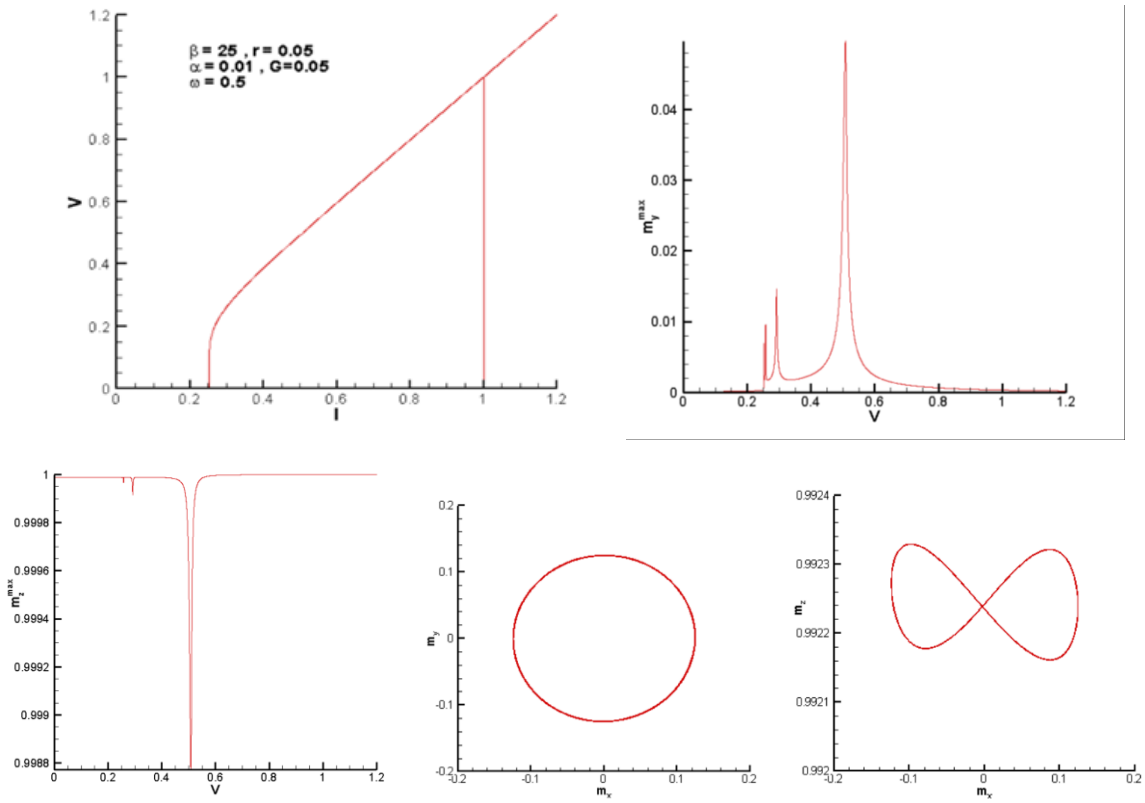

Figure 6: (a) IV characteristic of the Josephson junction. (b) (c) Plot of Ferromagnetic resonance in the voltage dependence of m_y^{max} & m_z^{max} (d) Magnetization trajectory in the $m_x - m_y$ plane at $I = 0.505$ corresponding to the max of the resonance curve, (e) similarly in $m_x - m_z$ plane.

Here, we calculated the temporal dependence of V and m_i at small dissipation $(\alpha << 1)$ for each value of bias current using C++ code. In Figure 6 (a), we observed the I-V characteristics graph at $\beta_c = 25$. Hysteresis is observed in the graph [12]. In Figure 6-(b),(c) presents the voltage dependence of the maximal amplitude of magnetic moment oscillations m_y^{max}, m_z^{max} taken in the time domain at each value of I calculated at small values of the Josephson to magnetic energy relation $G = 0.05$ and the spin-orbit coupling $r = 0.05$. In Figure 6 (d), we observe the $m_y - m_x$ plane's trajectory of magnetization at bias current $I = 0.505$ corresponding to the resonance peak. Similarly in (e), we observe for $m_z - m_x$, where small deviation to the y axis changes periodically during one rotation circle.

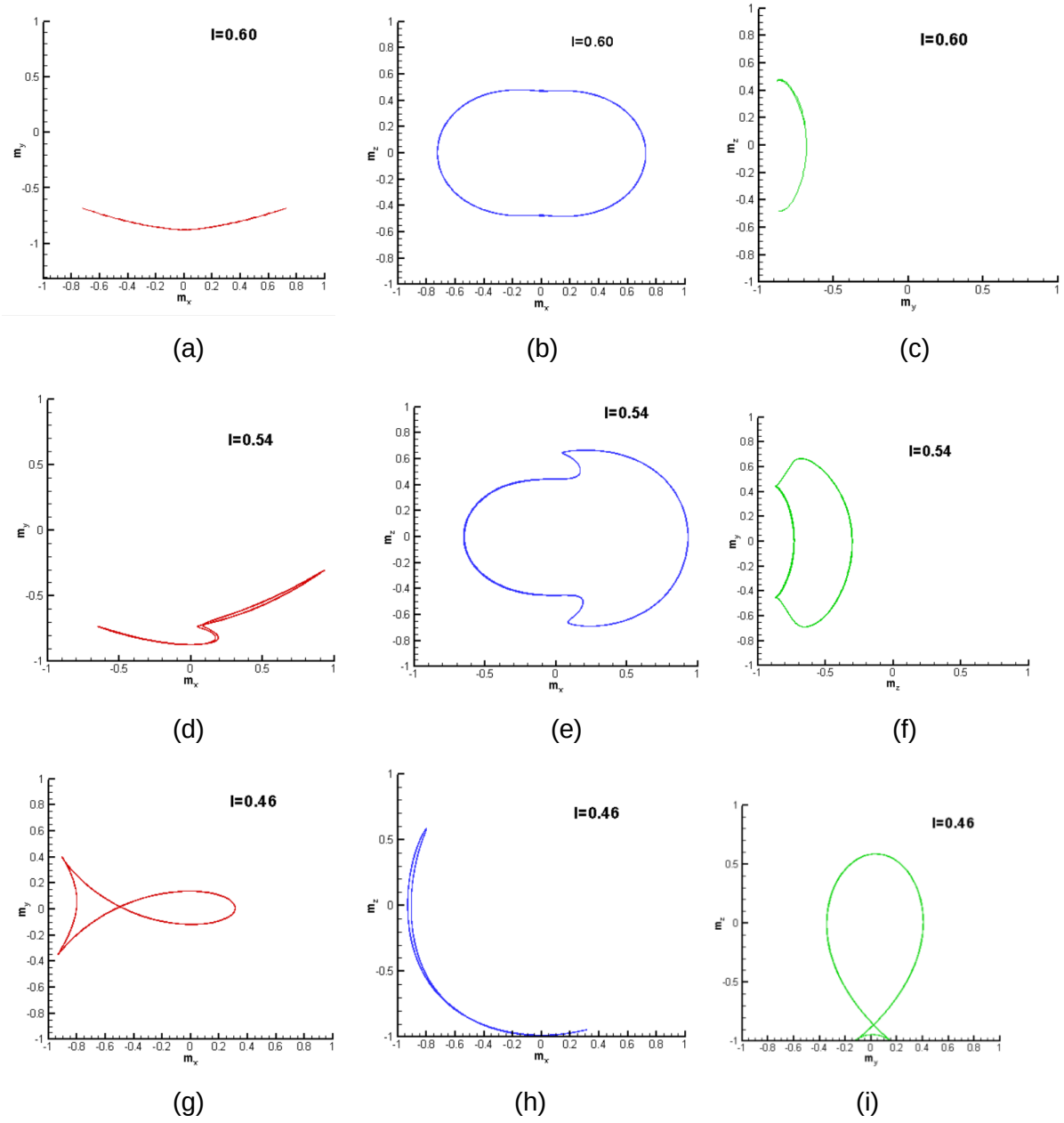

Figure 7: Magnetization trajectories in the planes $m_y - m_x$, $m_z - m_x$, $m_z - m_y$ for different I

We observed the specifi phase magnetization trajectories in the planes $m_y - m_x$, $m_z - m_x$, $m_z - m_y$ for different I, which were I=0.60, 0.54, 0.46. We observed different shapes for the magnetization trajectories which are plotted above. Some of the above shapes are also called with different names. For example, (b) is referred as 'apple, (d) as 'sickle', (e) as 'mushroom', (g) as fish. As we decreased the biasing current I, we observed as

cjhange in ‘moon’ to ‘mushroom’ trajectory in $m_z - m_x$ plane [12]. The above results presents a unique possibility of controlling the magnetization dynamics via external bias current I.

3. Conclusion

In this study, we first examined the superconductor-insulator-superconductor (SIS) Josephson Junction, with a current source driving a current through the junction and observed its properties. A C++ code was written to find the solution of second-order differential equation of Josephson Junction. For an underdamped Josephson junction, if the current is above I_c there will be resistance, but even if the current were to drop below I_c, there will still be resistance until the current has dropped off sufficiently. A hysteresis plot was observed. For overdamped Josephson junction, the solution will be imaginary for $I < I_c$ and linear and real for $I \gg I_c$. In presence of external radiation appearance of Shapiro steps was observed in superconducting materials, the width of those steps are strongly depend on the amplitude of these radiation. Later, we examined superconducting-ferromagnetic-superconducting (SFS) Josephson junction, and observed the magnetization dynamics using Landau-Lifshitz-Gilbert equation. A hysteresis was observed in the IVC. It was observed that for $m_z - m_x$, small deviation to the y axis changes periodically during one rotation circle. Overall SFS Josephson junctions have potential applications in superconducting electronics, such as qubits for quantum computing and spintronics and there is a scope for researchers to optimize and control the properties of the ferromagnetic layer more precisely.

4. Acknowledgment

I would like to express my sincere gratitude to my project supervisor, Dr. Majed Nashaat, for giving me the opportunity to work on this project and providing invaluable guidance throughout this project. I am grateful for his support, constant encouragement and for sharing his knowledge and experience with me. I would also like to thank the JINR Interest Team for their support and for this program that allows students from across the globe to utilize this opportunity and gain experience and knowledge. Special thanks to Prof. Yu. M. Shukrinov research group for providing the code for calculations.

5. References

[1] Philip W. Anderson, Physics Today 23, 11, 23 (1970); doi: 10.1063/1.3021826

[2] Giuliano, Domenico & Sodano, Pasquale. (2009). Pairing of Cooper pairs in a Josephson junction network containing an impurity. EPL (Europhysics Letters). 88. 10.1209/0295-5075/88/17012.

[3] Alexander V. Veretennikov, Valery V. Ryazanov, Supercurrents through the superconductor–ferromagnet–superconductor (SFS) junctions, Physica B: Condensed Matter, Volumes 284–288, Part 1, 2000.

[4] Shapovalov, A. & Febvre, Pascal & Yılmaz, Unal & Shnyrkov, V. I & Belogolovskii, Mikhail & Kordyuk, O. A. (2020). Low-Capacitance Josephson Junctions. Uspehi Fiziki Metallov. 21. 3-25. 10.15407/ufm.21.01.003.

[5] Bahrainirad, Ladan, "Josephson Currents In Two-Gap Superconductor-Insulator-Superconductor Junctions" (2013). Theses and Dissertations. 1395.

[6] Prof. Dr. Rudolf Gross and Dr. Achim Marx, Applied Superconductivity:
Josephson Effect and Superconducting Electronics, Manuscript to the Lectures during WS 2003/2004, WS 2005/2006, WS 2006/2007, WS 2007/2008, WS 2008/2009, and WS 2009/2010.

[7] Ponta, Linda & Carbone, Anna & Gilli, Marco. (2010). Resistive transition in disordered superconductors with varying intergrain coupling. Superconductor Science and Technology. 24. 10.1088/0953-2048/24/1/015006.

[8] Peder Heiselberg, Shapiro steps in Josephson Junctions, Niels Bohr Institute University of Copenhagen 12/6-13 (110291-3473)

[9] Rouzy, B. and Tollis, S. and Ivanov, D. A, Josephson current in a superconductor-ferromagnet junction with two noncollinear magnetic domains, 10.1103/PhysRevB.75.054503

[10] Shukrinov, Yu & Rahmonov, I. & Janalizadeh, A. & Kolahchi, M.. (2021). Anomalous Gilbert Damping and Duffing Features of the SFS φ_0 Josephson Junction.

[11] M. Lakshmanan, The Fascinating World of Landau-Lifshitz-Gilbert Equation

[12] Yu. M. Shukrinov, I. R. Rahmonov, and K. Sengupta, Ferromagnetic resonance and magnetic precessions in φ0 junctions, PHYSICAL REVIEW B 99, 224513 (2019)